

Entropy-Lens: The Information Signature of Transformer Computations

Riccardo Ali^{1*}, Francesco Caso^{2*}, Christopher Irwin^{3*}, Pietro Liò¹,

¹Department of Computer Science University of Cambridge
Cambridge, UK

²DIAG Sapienza University of Rome
Rome, Italy

³DISIT University of Eastern Piedmont
Alessandria, Italy

rma55@cam.ac.uk, francesco.caso@uniroma1.it, christopher.irwin@uniupo.it, pl219@cam.ac.uk

Abstract

Transformer models map input token sequences to output token distributions, layer by layer. While most interpretability work focuses on internal latent representations, we study the evolution of these token-level distributions directly in vocabulary space. However, such distributions are high-dimensional and defined on an unordered support, making common descriptors like moments or cumulants ill-suited. We address this by computing the Shannon entropy of each intermediate predicted distribution, yielding one interpretable scalar per layer. The resulting sequence—the *entropy profile*—serves as a compact, information-theoretic signature of the model’s computation.

We introduce Entropy-Lens, a model-agnostic framework that extracts entropy profiles from frozen, off-the-shelf transformers. We show that these profiles (i) reveal family-specific computation patterns invariant under depth rescaling, (ii) are predictive of prompt type and task format, and (iii) correlate with output correctness. We further show that Rényi entropies yield similar results within a broad range of α values, justifying the use of Shannon entropy as a stable and principled summary. Our results hold across different transformers, without requiring gradients, fine-tuning, or access to model internals.

1 Introduction

Transformer-based architectures (Vaswani et al. 2023) operate by iteratively mapping token inputs to distributions over next-token outputs, layer by layer (Shan et al. 2024). This view emphasizes their inherently probabilistic nature: each layer produces a distribution over the vocabulary, encoding the model’s beliefs at that stage.

Despite their success across domains—from language to biology to vision (Devlin 2018; Ji et al. 2021; Wu et al. 2020)—the internal evolution of these distributions remains poorly understood, resulting in unpredictable behaviour (Wei et al. 2022) and reliability concerns (Schroeder

and Wood-Doughty 2025; Huang et al. 2025). Most interpretability research either focuses on toy models (Elhage et al. 2021, 2022) or requires training a set of probes (nostalgia 2020; Belrose et al. 2023) or full models on ad-hoc tasks (Nanda et al. 2023), limiting scalability and generality. Moreover, existing methods primarily study latent representations—hidden states, attention maps, or MLP activations (Nanda and Bloom 2022; Bereska and Gavves 2024; Chefer, Gur, and Wolf 2021)—rather than the output distributions themselves. We propose to shift perspective: instead

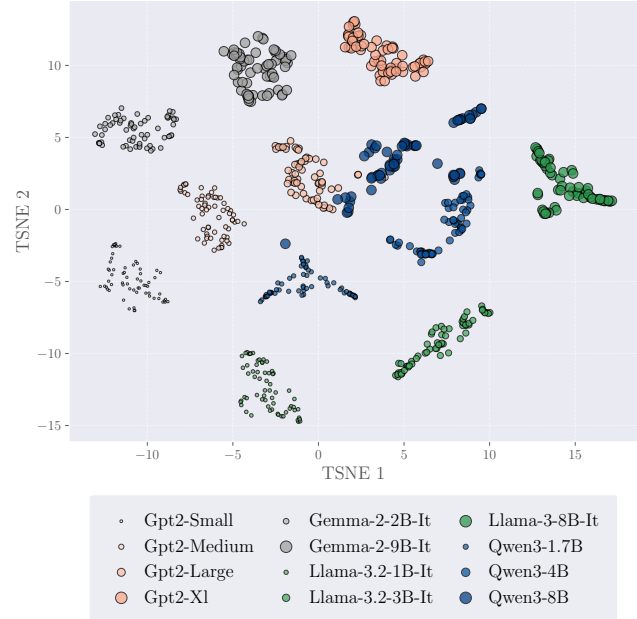


Figure 1: t-SNE of the aggregated entropy profiles of different model families using unprompted models. The size of each point is scaled based on the number of parameters of the model.

of analyzing the internal geometry of latent activations, we focus on the evolution of the model’s token-level predictions

*These authors contributed equally.

⁰Preprint - This manuscript is currently under review.

¹Code available at: github.com/christopher-irw/Entropy-Lens

across layers. These predictions, obtained by decoding intermediate representations via the model’s output head, form probability distributions over the vocabulary. Studying their evolution offers a direct, vocabulary-grounded view of the computation.

However, these distributions pose two challenges: they are high-dimensional (one value per token) and defined over an unordered support (the vocabulary). This makes classical descriptors like variance or higher-order cumulants unstable or ill-defined. We address both issues by computing the Shannon entropy of each distribution—a scalar, interpretable quantity invariant to token permutation, and reflective of the model’s uncertainty at each layer. We introduce Entropy-Lens, a simple, scalable, and model-agnostic framework for studying transformer computations through the evolution of entropy across layers.

In our experiments, we consider several LLMs, including Llama (Touvron et al. 2023), Gemma (Team et al. 2024), and GPT, (Radford 2018) up to 9B parameters. For each generated token, we compute the entropy of its intermediate predictions, as described in Section 4, yielding one interpretable value per layer: this constitutes the *entropy profile*. We then aggregate these profiles across tokens and study whether they capture structural information about the internal LLM’s computation (Figure 1). In Section 5, we show that: (i) entropy profiles reveal family-specific signatures of transformer architectures, invariant under depth rescaling; (ii) they are predictive of prompt semantics and format; (iii) they correlate with output correctness; (iv) and results are stable across Rényi entropy variants, justifying our use of Shannon entropy as a principled default.

Entropy-Lens requires no gradients, no fine-tuning, and no access to internal weights. It applies to frozen, off-the-shelf transformers of arbitrary size. While our experiments focus on language models, the methodology is general and opens new directions for vocabulary-grounded interpretability.

2 Related Work

Lenses in LLMs Mechanistic interpretability (Bereska and Gavves 2024) aims to provide a precise description and prediction of transformer-based computations. Common tools in the field are *lenses*, which are a broad class of probes deployed in intermediate steps of the residual stream. For example, logit-lens (nostalgebrist 2020) uses the model’s decoder function to decode the intermediate activations in the vocabulary space. tuned-lens (Belrose et al. 2023) refines this technique by training a different affine probe at each layer, instead of only using the pretrained model’s decoder function. Building on the Transformer-Lens library (Nanda and Bloom 2022), we propose Entropy-Lens, which employs logit-lens to study and characterize LLMs’ computations via their decoded version with information theory.

Information theory in Transformers Information theory has been studied both in connection to the training phase of LLMs and their interpretability. For example, a collapse in attention entropy has been linked to training instabilities (Zhai et al. 2023) and matrix entropy was employed to evaluate “compression” in LLMs (Wei et al. 2024). Additionally, mutual information was used to study the effectiveness of the chain-of-thought mechanism (Ton, Taufiq, and Liu 2024). Our work, instead, shifts the focus on the vocabulary’s natural domain. Through Entropy-Lens, we use information theory to study the evolution of entropy of the intermediate layers’ decoded logits. A related study by Dombrowski and Corlouer (2024) uses information-theoretic measures to distinguish between truthful and deceptive LLM generations. Their analysis focuses on deception under explicit instruction, whereas our work aims at uncovering broader entropy-based signatures across model families, prompt types, and output correctness without requiring behavioral framing or fine-tuned prompting.

3 Background

3.1 Information theory

The main information-theoretic quantity used in our study is *entropy*. Given a discrete² random variable X with outcomes x_i and probability mass function p , the *Shannon entropy* H of X is defined as

$$H(X) = - \sum_i p(x_i) \log p(x_i) = \mathbb{E}[-\log p(X)] \quad (1)$$

Shannon proved that this function is the only one—up to a scalar multiplication—that satisfies intuitive properties for measuring ‘disorder’ (Shannon 1948). These include being maximal for a uniform distribution, minimal for the limit of a Kronecker delta function, and ensuring that $H(A, B) \leq H(A) + H(B)$ for every possible event A and B . The same function already existed in continuous form in physics, where it linked the probabilistic formalism of statistical mechanics with the more phenomenological framework of thermodynamics, where the term ‘entropy’ was originally coined (Gibbs 1902). In addition to Shannon entropy, we also consider its generalization known as *Rényi entropy*. Given a discrete random variable X with probability mass function p , the Rényi entropy of order $\alpha > 0, \alpha \neq 1$, is defined as:

$$H_\alpha(X) = \frac{1}{1-\alpha} \log \sum_i p(x_i)^\alpha \quad (2)$$

This formulation reduces to Shannon entropy in the limit $\alpha \rightarrow 1$, and introduces a tunable parameter α that modulates the sensitivity of the entropy to the distribution’s tail. Lower values of α give more weight to rare events, while higher values emphasize the most probable outcomes. Next, we study the entropy of vocabulary predictions—a quantity that is maximal when the prediction assigns equal probability to all tokens, minimal when it assigns zero probability to all but one token, and takes intermediate values when probability is distributed across multiple tokens, consistent with the previously mentioned properties. In our experiments, we explored a range of α values to understand

²Although entropy can be naturally extended to the continuous case with probability *density* functions, we restrict ourselves to the discrete case as it is the most relevant to our study.

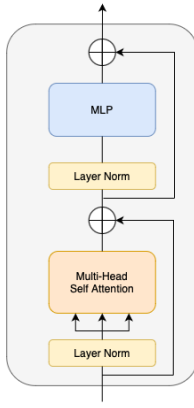


Figure 2: Structure of a generic Transformer block.

how this parameter affects the informativeness of the resulting entropy profiles. We identified an *informative range* of α values—which includes the Shannon case $\alpha = 1$ —where entropy profiles retain high discriminative power for classification tasks. Outside of this range, we observe that profiles tend to collapse: for very small α , entropies become nearly maximal and lose contrast across layers and examples; for large α , they become very small and overly sensitive to noise and local fluctuations. These findings support the use of Shannon entropy as a balanced and parameter-free choice, robust across a wide range of practical conditions.

3.2 The Transformer

Architecture The transformer (Vaswani et al. 2023) is a deep learning architecture widely applied in language modelling with LLMs (Brown et al. 2020) and computer vision (Dosovitskiy et al. 2021). Transformer computations happen through *transformer blocks* and *residual connections*, as exemplified in Figure 3. While various design choices are possible, blocks are usually a composition of layer normalization (Zhang and Sennrich 2019), attention, and multi layer perceptrons (MLPs), as shown in Figure 2. Residual connections, instead, sum the output of the layer $i - 1$ to the output of the layer i .

Inside a single transformer block, the information flows both *horizontally* and *vertically*. The former, enabled by the attention mechanism, allows the token representations to interact with each other. In a language modelling task, for example, this is useful to identify which parts of the input sequence—the sentence prompt—should influence the next token prediction and quantify by how much. The latter vertical information flow allows the representation to evolve and encode different meanings or concepts. Usually, the dimension of the latent space is the same for each block in the transformer. The embedding spaces where these computations take place are generally called the *residual stream*.

Computation schema LLMs are trained to predict the next token in a sentence. That is, given a sentence prompt S with tokens t_1, \dots, t_N , the transformer encodes each token with a linear encoder E . Throughout the residual stream,

the representation x_N of the token t_N evolves into the representation of the token t_{N+1} , which is then decoded back into token space via a linear decoder D , often set to E^\top , tying the embedding weights and the decoder. Finally, the logits—the output of D —are normalized with softmax to represent a probability distribution over the vocabulary. We summarize this operation with the function $W := \text{softmax} \circ D$.

In formal terms, information processing can be expressed using the encoder, decoder, Transformer block f , and residual connection:

$$x_j^0 = E(t_j) \quad (3)$$

$$x_j^i = f^i(x_j^{i-1}) + x_j^{i-1} \quad (4)$$

$$y_j^i = W(x_j^i) \quad (5)$$

where $j \in \{1, \dots, N\}$ ranges over the number of tokens in the prompt and $i \in \{0, \dots, L\}$ ranges over the number of layers. Hence, x_j^i represents the activations of token t_j after layer i .

Instruct models Training an LLM requires vast amounts of data and is generally divided into multiple phases.

- **Pretraining:** The model is exposed to large datasets through self-supervised tasks, such as next-token prediction or similar variants. This phase helps the model learn a broad range of general knowledge.
- **Fine-tuning:** This phase teaches the model to generate more useful and coherent responses. Two main strategies are used: *Chat*: The model is trained on structured conversations between a user and the model, with clearly defined roles. *Instruct*: The model learns from simple commands, without a predefined dialogue structure.
- **RLHF (optional):** Some models undergo Reinforcement Learning from Human Feedback (RLHF) to further refine their responses based on human preferences.

For our experiments, we used off-the-shelf models without RLHF to analyze information processing in a less biased transformer version. We also focused on Instruct models (abbreviated with *it* in tables and figures) instead of Chat models for two reasons: 1. the Instruct strategy aligns better with our experimental setup 2. Instruct models are more flexible and often preferred for practical applications.

4 Method

Entropy-Lens’s pipeline comprises three steps and is described in Figure 3. After introducing the notation and motivating the choice of entropy as a measure, in the following we describe the details of the framework which as been used for the experiments in the following sections.

Notation We denote the input sentence comprising tokens t_1, \dots, t_N by $S = (t_i)_{i=1}^N$. Then, x_j^i denotes the activations of the token t_j after block i for $j \in \{1, \dots, N\}$ and $i \in \{1, \dots, L\}$. Since our analysis focuses on the logits extracted from the intermediate layers of the transformer, it will be useful to distinguish between *normalized* and *unnorma-*
lized logits. We define $W := \text{softmax} \circ D$ and $y_j^i := W(x_j^i)$ the normalized logits of the token t_j ’s activations after layer i .

Why entropy? Our goal is to characterize how a transformer model evolves its predictions across layers, remaining in the token space for interpretability. Each intermediate representation, once decoded and passed through softmax, yields a probability distribution over the vocabulary. However, this distribution lives on a high-dimensional, unordered categorical support.

Classical descriptors such as variance or higher-order cumulants rely on an implicit ordering of the support and thus become meaningless when applied to token distributions—shuffling token indices alters their value arbitrarily. Entropy, on the other hand, is invariant under permutations and captures a well-defined notion of uncertainty or informativeness regardless of vocabulary indexing. It is therefore a natural and stable choice to summarize the evolution of token-level beliefs across transformer layers.

Definitions The core of our methodology is to analyze the entropy of the generated tokens’ intermediate representations y_j^i . These vectors are probability distributions, as they are the output of a softmax. To obtain a single quantity that summarizes the information they contain, we compute their entropy $H(y_j^i)$. For one generated token, we can consider the entropy of all of its intermediate predictions $H(y_j^i)$ for $i \in \{1, \dots, L\}$. This leads us to the definition of entropy profile:

Definition 1 (Entropy profile) Let $h_j^i = H(y_j^i)$ be the entropy of the intermediate representation of token t_j after block i and residual connection. The entropy profile of the next generated token is defined as

$$h_N = \bigoplus_i h_N^i \quad (6)$$

where \bigoplus denotes any aggregation function.

In our experiments, we set \bigoplus to be concatenation, so that $h_N = (h_N^1, \dots, h_N^L)^\top$, but other choices are possible. The extraction of entropy profiles is the step 1 of our pipeline.

Then, we fix the number of tokens that the LLM is required to generate, T and repeat the same procedure for each of them, leading us to the next definition:

Definition 2 (Aggregated entropy profile) Let h_{N+t} be the entropy profiles according to Definition 1 for $t \in \{0, \dots, T-1\}$, i.e. the entropy profile of each token generated sequentially by a transformer. The aggregated entropy profile of the next T generated tokens is defined as

$$h_{[N:T]} = \bigotimes_{t=0}^{T-1} h_{N+t} \quad (7)$$

where \bigotimes denotes any aggregation function.

Note that \bigotimes in Definition 2 need not be the same as \bigoplus in Definition 1. In our experiments, we set both of them to be concatenation, so that $h_{[N:T]}$ is the matrix with h_{N+t} as columns, that is $(h_{[N:T]})_t^i = h_{N+t}^i$ for $i \in \{1, \dots, L\}$ and $t \in \{0, \dots, T-1\}$. The aggregation of entropy profiles is the step 2 of our framework.

The last step of our framework is classification, where we feed the aggregated entropy profile to a classifier \mathcal{C} to determine whether it contains sufficient information to identify a particular ‘entity’. In our experiments, we take \mathcal{C} to be a k-NN classifier.

We also examine whether aggregated entropy profiles identify model family (Section 5.1), task type and format (Sections 5.2 and 5.5), and correct and wrong answers to multiple choice questions (Section 5.3) in LLMs.

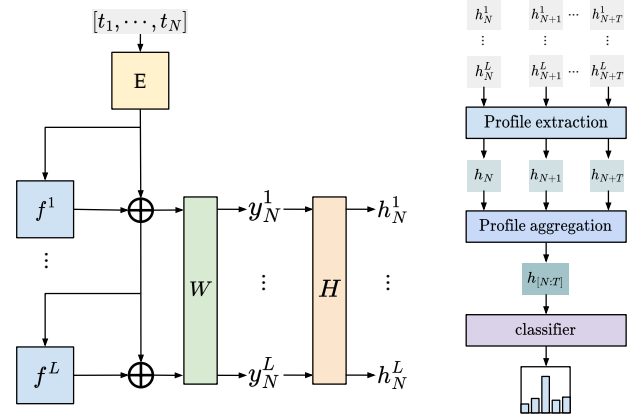


Figure 3: Entropy-Lens’s pipeline. (Left) A diagram representing a transformer architecture: hidden representations are converted into intermediate predictions with W before calculating their entropy H . (Right) A diagram representing our framework: step 1: entropy profile extraction, step 2: entropy profile aggregation and step 3: classification.

5 Experiments

Our experiments focus on several key aspects. First, we show that entropy profiles are indicative of model family, with distinctions becoming more pronounced as model size increases. We then investigate whether a model’s entropy profile alone can be used to classify the task it is performing. Next, we assess whether entropy profiles capture information about output formatting, independently of task content. We extend this analysis to evaluate whether entropy profiles can distinguish between correct and incorrect task execution. Additionally, we explore the effect of varying the alpha parameter in Rényi entropy, examining how it influences the expressiveness of the resulting profiles.

5.1 Entropy profiles identify model families

We assess whether aggregated entropy profiles can distinguish different model families by visualizing and analyzing those of 12 models from 4 different families (GPT, Gemma, LLaMA and Qwen) with parameter counts ranging from 100M to 9B.

We average 64 entropy profiles obtained by generating 32 tokens prompting the model with a completely blank prompt. We observe (see Figure 1) that the profiles relate uniquely to the model family, rather than a particular model, independently of its size. Moreover, we observe that each

model size within a particular family is tied to a scaling factor if we normalize by number of layers (see Figure 4).

The GPT model class starts with high vocabulary entropy in the early layers, indicating a wide range of possible response tokens. Then, entropy gradually decreases—more smoothly than in other classes—leading to a low-entropy state, where the model narrows down to a small set of possible response tokens.

The Gemma model class, on the other hand, starts with high entropy in the very first layer, then sharply drops to lower entropy, rises again in the intermediate layers, and finally decreases to low entropy again just before the last layers, where the model is required to produce an output token.

The Llama model class starts with low entropy, then steeply rises and maintains a high entropy value over a large range of intermediate layers, finally decreasing to low entropy again.

The Qwen model family exhibits a similar trend, but in a more gradual manner, resulting in less well-defined regimes.

We observe that the equivalence between models of the same family but different sizes holds when looking at the entropy trend not as a function of the absolute layer index, but rather as the relative layer position within the model.

We conjecture that high entropy phases, whether in the early or intermediate layers, allow the model to explore more possibilities in its response, similarly to how temperature helps avoid getting stuck in local minima in optimization. Then, at the moment of selection, the distribution is ‘cooled down’, forcing the output to be limited to a few possible tokens.

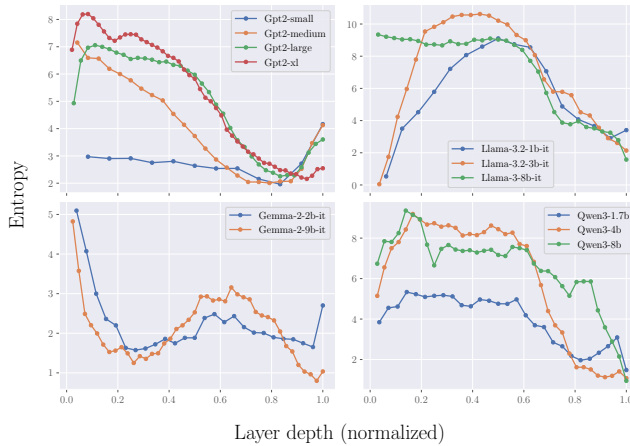


Figure 4: Average of 64 entropy profiles over 32 generated tokens per model. The x axis is normalized for an easier comparison when models have a different number of layers.

5.2 Entropy profiles identify task types

We verify whether the entropy profiles can identify task types examining generative (continue a text), syntactic (count the number of words in a text), and semantic (extract the subject or moral of a text) tasks.

We do this with the *TinyStories* dataset (Eldan and Li 2023). For evaluation robustness, we construct for each task

type three prompt templates using a combination of task-specific task prompts, reported in Appendix C.1 Table 4, and a story from *TinyStories*. These templates are:

- **Base**, of the form task prompt + story
- **Reversed**, of the form story + task prompt
- **Scrambled**, of the form task prompt + scrambled story or scrambled story + task prompt, at random. A scrambled story is a ‘story’ obtained by randomly shuffling the words in a given story from *TinyStories*.

Note that, for a robust evaluation, we also use 2 possible task prompt variations, as per Table 4.

We generate 800 prompts per task type, 1/3 of them with the base template, 1/3 with the reversed template, and 1/3 with the scrambled templates, for a total of 2400 prompts. We then apply our pipeline from Section 4 to classify the aggregated entropy profiles of these prompts against their task type using a k-NN classifier. The model was evaluated in a 10-fold cross-validation using the ROC-AUC score (one-vs-rest), a standard choice for measuring classification performance. Table 1 shows the results obtained for 6 models with parameter counts ranging from 1B to 9B. Figure 5 shows the average entropy profiles per task type.

We observe that all k-NN classifiers (i.e. one for each LLM) achieve high accuracy in distinguishing entropy profiles, with a trend toward improved performance for larger models.

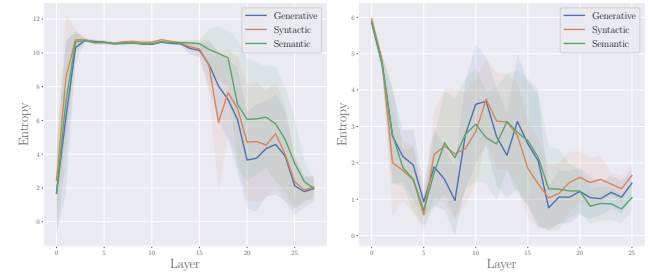


Figure 5: Average entropy profiles with shaded standard deviation for different task types: generative, syntactic, and semantic. These tasks are induced with the prompts described in Appendix C.1. Left: Llama-3.2-it. Right: Gemma-2-it.

Model	Model Size	k-NN ROC-AUC
Gemma-2-it	2.1B	97.66 ± 0.47
Gemma-2-it	8.9B	98.38 ± 0.50
Llama-3.2-it	1 B	94.94 ± 0.79
Llama-3.2-it	3 B	94.77 ± 0.93
Llama-3-it	8 B	96.10 ± 0.67
Phi-3	3.6B	97.07 ± 0.87

Table 1: ROC-AUC (one-vs-rest) results of different models on the *TinyStories* task classification. Standard deviations are computed over 10-fold cross-validation splits.

5.3 Entropy profiles identify correct task execution

We test whether entropy profiles can identify correct and wrong answers generated by LLMs using the Massive Multi-task Language Understanding (MMLU) dataset (Hendrycks et al. 2021). MMLU consists of multiple-choice questions across 57 subjects, ranging from history and physics to law, mathematics, and medicine. The difficulty levels span from elementary to professional, making it a benchmark for evaluating language models on specialized domains. Each dataset entry contains: a question string, four answer choices and a label indicating the correct answer.

We evaluate two models, a Llama-3.2 with 3B parameters Instruct and a Gemma-2 with 2B parameters, by presenting the multiple-choice questions in three different formats (as per Table 5 in Appendix C.2):

- **Base:** A minimal version containing the topic, the question, and multiple-choice answers.
- **Instruct:** A version with a brief explanation that it’s a multiple-choice test where only one option should be selected.
- **Humble:** A version that also instructs the model to pick a completely random option if it doesn’t know the answer.

Then, we apply our pipeline to extract and aggregate the responses’ entropy profiles and classify them against the correctness of the corresponding LLM-generated answer. We train a k-NN classifier for each LLM and validate it using 10-fold cross-validation. We also conduct a t-test to compare our classifier to a dummy model. This dummy model generates predictions randomly, sampled from a distribution that reflects the proportion of correct and incorrect answers produced by the LLM, ensuring robustness against class imbalance. The results reject the null hypothesis ($\alpha = 0.05$) with the k-NN achieving an AUC-ROC between 67.23 and 73.61, depending on prompt type and model (see Table 3).

We observe that the instruct and humble prompts improve Llama’s average accuracy, while for Gemma, this is only true for the instruct prompt. Additionally, in Llama, the model’s higher accuracy seems to be partially linked to greater difficulty in distinguishing correct from incorrect entropy profiles, though more rigorous analysis is needed to confirm this. In Gemma, however, this claim is harder to support.

5.4 Three regimes of Rényi entropy

To qualitatively explore how the Rényi entropy affects the structure of entropy profiles, we compute pairwise cosine similarities between profiles generated with different values of α . This analysis is performed on a subset of the *topic-format* dataset, and the resulting similarity matrices are shown in Figure 7.

We observe three distinct regimes as α varies:

- For very small values of α (e.g., $\alpha < 0.2$), the similarity matrices are nearly flat, with profiles being almost identical across examples. This is expected, as Rényi entropy in this regime weights all tokens with non-zero probability almost equally, and usually all tokens have non-null probability.

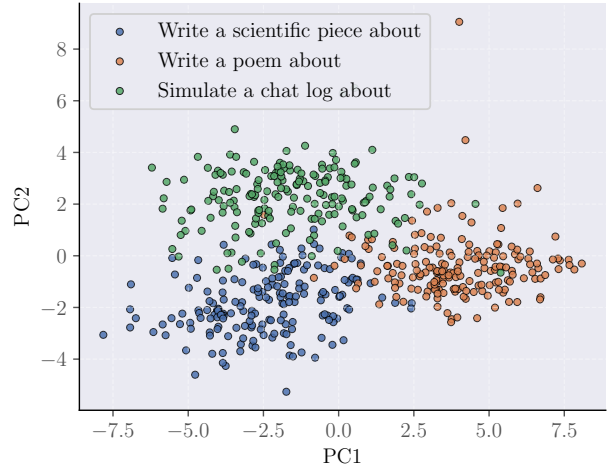


Figure 6: PCA projection on aggregated entropy profiles extracted from the *topic-format* dataset.

- For large values of α (e.g., $\alpha > 20$), the similarity matrices also flatten. In this case, the entropy becomes increasingly dominated by the few tokens with highest probabilities. Since these sets of top tokens tend to have similar cardinalities (in the limit equal to 1), the profiles collapse into a narrow set of values, losing expressiveness and becoming more sensitive to local fluctuations.
- Between these extremes lies an informative regime—approximately $0.5 \leq \alpha \leq 20$ —where entropy profiles are heterogeneous enough to retain meaningful variation. This is reflected in the standard deviation of the similarity matrices, which peaks in this interval.

This qualitative observation supports our empirical findings: in Section 5.5, we show that format classification accuracy remains high and stable within this informative α range. Notably, Shannon entropy ($\alpha = 1$) falls within this interval, providing a strong justification for its use in the main experiments. By choosing $\alpha = 1$, we retain discriminative power while avoiding the need to tune additional hyperparameters.

5.5 Entropy profiles identify text format

We test whether the entropy profiles contain signal about the *format* of the generated text. In this experiment, we prompt the model to produce short texts across different topics while enforcing one of three predefined formats: poem, scientific piece, or chat log. We call these generated texts the *topic-format* dataset. We use entropy profiles computed not only with Shannon entropy ($\alpha = 1$), but also with Rényi entropy for $\alpha \in \{0.5, 5.0\}$. As shown in Table 2, the k-NN classifier achieves high ROC-AUC scores across all values of α , indicating that the format is reliably encoded in the entropy profiles. Moreover, the small variability in performance across α values supports our use of Shannon entropy as a principled, parameter-free default.

To better understand the structure of the entropy profiles, we perform Principal Component Analysis (PCA) and vi-

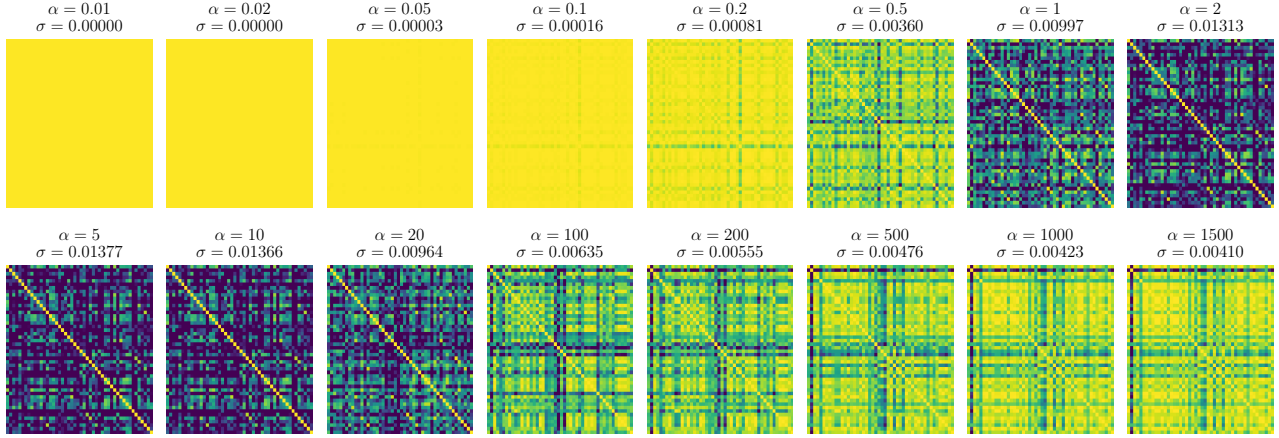


Figure 7: Cosine similarity matrices between entropy profiles computed on a subset of the *topic-format* dataset using different values of α in the Rényi entropy. σ denotes the standard deviation of the similarity matrix. Note how similarity flattens for very low and very high α , while intermediate values yield more informative profiles.

Model	α	k-NN ROC-AUC
Gemma-2-2b-it	0.5	97.3 ± 1.6
	1.0	98.7 ± 1.1
	5.0	98.4 ± 1.7
Llama-3.2-1b-it	0.5	97.8 ± 1.6
	1.0	97.8 ± 2.4
	5.0	96.6 ± 2.6

Table 2: ROC-AUC (one-vs-rest) results of two models with three values of α for the Rényi entropy for format classification. Standard deviations are computed over 10-fold cross-validation splits.

sualize the first two components. As shown in Figure 6, the profiles cluster distinctly by format, forming linearly separable groups in the reduced space. This indicates that format-specific computation patterns are not only detectable by a classifier, but visibly reflected in the global shape of the entropy evolution across layers.

Model	Prompt	LLM Acc.	k-NN AUC-ROC
Llama	Base	50.89	73.61 ± 1.52
	Humble	58.51	69.90 ± 1.06
	Instruct	60.62	67.23 ± 1.62
Gemma	Base	56.10	71.88 ± 1.63
	Humble	54.71	72.78 ± 1.15
	Instruct	56.38	68.36 ± 1.23

Table 3: Performance comparison of two models (Llama-3.2-3B-it and Gemma-2-2B-it) for different prompt types on MMLU accuracy and k-NN AUC-ROC score.

6 Conclusions

In this work, we prototyped a novel model-agnostic interpretability framework for large-scale transformer-based architectures grounded in information-theory. In Section 5.1, we showed that the entropy profiles of LLM intermediate predictions identify the LLM’s model family. Additionally, in Sections 5.2 and 5.5 we showed that the same entropy profiles can be used to identify the ‘task type’ and the ‘format type’ in LLMs, whilst in Section 5.3 we used them to distinguish between correct and wrong LLM generated answers. Moreover, we investigated the validity of using Shannon entropy instead of the more general Rényi entropy, and empirically demonstrated its effectiveness. Importantly, all our experiments were conducted on frozen off-the-shelf large-scale transformers.

6.1 Limitations and Future Work

While this work paves the way to further investigations in information theoretic interpretability, it also presents a number of limitations. First, the concepts of ‘task type’ and ‘format type’ don’t have a formal and well established definition.

Moreover, we showed how different models possess different characteristic entropy profiles. We conjecture that these particular shapes are a byproduct of training procedure and architectural designs, but future research could focus on understanding the precise connections. Currently, we do not have a theoretical explanation for the observed phenomena or their underlying causes.

Another interesting line of research could focus on considering more fine-grained measures of information instead of just an aggregated one such as entropy.

With these limitations in mind, our methodology could be used to probe the reasoning capabilities of LLMs, for instance by comparing the entropy profile of a reasoning task vs. a data retrieval task. If these profiles happen to match, it could be taken as an argument against the ability of LLMs to reason. Conversely, if they do not, it may suggest that some form of reasoning is indeed occurring.

Finally, recent literature explored the use of entropy for private inference (PI), where computations are performed on encrypted data without revealing users' sensitive information (Jha and Reagen 2025). While previous work focused on the entropy of the attention mechanism, future research could use our methodology to develop PI-friendly applications of LLMs.

References

Belrose, N.; Furman, Z.; Smith, L.; Halawi, D.; Ostrovsky, I.; McKinney, L.; Biderman, S.; and Steinhardt, J. 2023. Eliciting Latent Predictions from Transformers with the Tuned Lens. *arXiv:2303.08112*.

Bereska, L.; and Gavves, E. 2024. Mechanistic Interpretability for AI Safety – A Review. *arXiv:2404.14082*.

Brown, T. B.; Mann, B.; Ryder, N.; Subbiah, M.; Kaplan, J.; Dhariwal, P.; Neelakantan, A.; Shyam, P.; Sastry, G.; Askell, A.; Agarwal, S.; Herbert-Voss, A.; Krueger, G.; Henighan, T.; Child, R.; Ramesh, A.; Ziegler, D. M.; Wu, J.; Winter, C.; Hesse, C.; Chen, M.; Sigler, E.; Litwin, M.; Gray, S.; Chess, B.; Clark, J.; Berner, C.; McCandlish, S.; Radford, A.; Sutskever, I.; and Amodei, D. 2020. Language Models are Few-Shot Learners. *arXiv:2005.14165*.

Chefer, H.; Gur, S.; and Wolf, L. 2021. Transformer Interpretability Beyond Attention Visualization. *arXiv:2012.09838*.

Devlin, J. 2018. Bert: Pre-training of deep bidirectional transformers for language understanding. *arXiv preprint arXiv:1810.04805*.

Dombrowski, A.-K.; and Corlouer, G. 2024. An information-theoretic study of lying in LLMs. In *ICML 2024 Workshop on LLMs and Cognition*.

Dosovitskiy, A.; Beyer, L.; Kolesnikov, A.; Weissenborn, D.; Zhai, X.; Unterthiner, T.; Dehghani, M.; Minderer, M.; Heigold, G.; Gelly, S.; Uszkoreit, J.; and Houlsby, N. 2021. An Image is Worth 16x16 Words: Transformers for Image Recognition at Scale. *arXiv:2010.11929*.

Eldan, R.; and Li, Y. 2023. Tinystories: How small can language models be and still speak coherent english? *arXiv preprint arXiv:2305.07759*.

Elhage, N.; Hume, T.; Olsson, C.; Schiefer, N.; Henighan, T.; Kravec, S.; Hatfield-Dodds, Z.; Lasenby, R.; Drain, D.; Chen, C.; Grosse, R.; McCandlish, S.; Kaplan, J.; Amodei, D.; Wattenberg, M.; and Olah, C. 2022. Toy Models of Superposition. *Transformer Circuits Thread*. Https://transformercircuits.pub/2022/toy_model/index.html.

Elhage, N.; Nanda, N.; Olsson, C.; Henighan, T.; Joseph, N.; Mann, B.; Askell, A.; Bai, Y.; Chen, A.; Conerly, T.; DasSarma, N.; Drain, D.; Ganguli, D.; Hatfield-Dodds, Z.; Hernandez, D.; Jones, A.; Kernion, J.; Lovitt, L.; Ndousse, K.; Amodei, D.; Brown, T.; Clark, J.; Kaplan, J.; McCandlish, S.; and Olah, C. 2021. A Mathematical Framework for Transformer Circuits. *Transformer Circuits Thread*. <Https://transformercircuits.pub/2021/framework/index.html>.

Gibbs, J. W. 1902. *Elementary principles in statistical mechanics: developed with especial reference to the rational foundations of thermodynamics*. C. Scribner's sons.

Hendrycks, D.; Burns, C.; Basart, S.; Zou, A.; Mazeika, M.; Song, D.; and Steinhardt, J. 2021. Measuring Massive Multitask Language Understanding. *arXiv:2009.03300*.

Huang, L.; Yu, W.; Ma, W.; Zhong, W.; Feng, Z.; Wang, H.; Chen, Q.; Peng, W.; Feng, X.; Qin, B.; and Liu, T. 2025. A Survey on Hallucination in Large Language Models: Principles, Taxonomy, Challenges, and Open Questions. *ACM Transactions on Information Systems*, 43(2): 1–55.

Jha, N. K.; and Reagen, B. 2025. Entropy-Guided Attention for Private LLMs. *arXiv:2501.03489*.

Ji, Y.; Zhou, Z.; Liu, H.; and Davuluri, R. V. 2021. DNABERT: pre-trained Bidirectional Encoder Representations from Transformers model for DNA-language in genome. *Bioinformatics*, 37(15): 2112–2120.

Nanda, N.; and Bloom, J. 2022. TransformerLens. <https://github.com/TransformerLensOrg/TransformerLens>.

Nanda, N.; Chan, L.; Lieberum, T.; Smith, J.; and Steinhardt, J. 2023. Progress measures for grokking via mechanistic interpretability. *arXiv:2301.05217*.

nostalgebraist. 2020. interpreting gpt: the logit-lense. <https://www.lesswrong.com/posts/AcKRB8wDpdAN6v6ru/interpreting-gpt-the-logit-lens>. Accessed: 17-02-2025.

Radford, A. 2018. Improving language understanding by generative pre-training.

Russakovsky, O.; Deng, J.; Su, H.; Krause, J.; Satheesh, S.; Ma, S.; Huang, Z.; Karpathy, A.; Khosla, A.; Bernstein, M.; Berg, A. C.; and Fei-Fei, L. 2015. ImageNet Large Scale Visual Recognition Challenge. *International Journal of Computer Vision (IJCV)*, 115(3): 211–252.

Schroeder, K.; and Wood-Doughty, Z. 2025. Can You Trust LLM Judgments? Reliability of LLM-as-a-Judge. *arXiv:2412.12509*.

Shan, W.; Meng, L.; Zheng, T.; Luo, Y.; Li, B.; Xiao, T.; Zhu, J.; et al. 2024. Early Exit Is a Natural Capability in Transformer-based Models: An Empirical Study on Early Exit without Joint Optimization. *arXiv preprint arXiv:2412.01455*.

Shannon, C. E. 1948. A mathematical theory of communication. *The Bell system technical journal*, 27(3): 379–423.

Team, G.; Mesnard, T.; Hardin, C.; Dadashi, R.; Bhupatiraju, S.; Pathak, S.; Sifre, L.; Rivière, M.; Kale, M. S.; Love, J.; Tafti, P.; Husseinot, L.; Sessa, P. G.; Chowdhery, A.; Roberts, A.; Barua, A.; Botev, A.; Castro-Ros, A.; Slone, A.; Héliou, A.; Tachetti, A.; Bulanova, A.; Peterson, A.; Tsai, B.; Shahriari, B.; Lan, C. L.; Choquette-Choo, C. A.; Crepy, C.; Cer, D.; Ippolito, D.; Reid, D.; Buchatskaya, E.; Ni, E.; Noland, E.; Yan, G.; Tucker, G.; Muraru, G.-C.; Rozhdestvenskiy, G.; Michalewski, H.; Tenney, I.; Grishchenko, I.; Austin, J.; Keeling, J.; Labanowski, J.; Lespiau, J.-B.; Stanway, J.; Brennan, J.; Chen, J.; Ferret, J.; Chiu, J.; Mao-Jones, J.; Lee, K.; Yu, K.; Millican, K.; Sjoesund, L. L.; Lee, L.; Dixon, L.; Reid, M.; Mikuła, M.; Wirth, M.; Sharman, M.; Chinaev, N.; Thain, N.; Bachem,

O.; Chang, O.; Wahltinez, O.; Bailey, P.; Michel, P.; Yotov, P.; Chaabouni, R.; Comanescu, R.; Jana, R.; Anil, R.; McIlroy, R.; Liu, R.; Mullins, R.; Smith, S. L.; Borgeaud, S.; Girgin, S.; Douglas, S.; Pandya, S.; Shakeri, S.; De, S.; Klimenko, T.; Hennigan, T.; Feinberg, V.; Stokowiec, W.; hui Chen, Y.; Ahmed, Z.; Gong, Z.; Warkentin, T.; Peran, L.; Giang, M.; Farabet, C.; Vinyals, O.; Dean, J.; Kavukcuoglu, K.; Hassabis, D.; Ghahramani, Z.; Eck, D.; Barral, J.; Pereira, F.; Collins, E.; Joulin, A.; Fiedel, N.; Senter, E.; Andreev, A.; and Kenealy, K. 2024. Gemma: Open Models Based on Gemini Research and Technology. arXiv:2403.08295.

Ton, J.-F.; Taufiq, M. F.; and Liu, Y. 2024. Understanding Chain-of-Thought in LLMs through Information Theory. arXiv:2411.11984.

Touvron, H.; Lavril, T.; Izacard, G.; Martinet, X.; Lachaux, M.-A.; Lacroix, T.; Rozière, B.; Goyal, N.; Hambro, E.; Azhar, F.; Rodriguez, A.; Joulin, A.; Grave, E.; and Lample, G. 2023. LLaMA: Open and Efficient Foundation Language Models. arXiv:2302.13971.

Vaswani, A.; Shazeer, N.; Parmar, N.; Uszkoreit, J.; Jones, L.; Gomez, A. N.; Kaiser, L.; and Polosukhin, I. 2023. Attention Is All You Need. arXiv:1706.03762.

Wei, J.; Tay, Y.; Bommasani, R.; Raffel, C.; Zoph, B.; Borgeaud, S.; Yogatama, D.; Bosma, M.; Zhou, D.; Metzler, D.; Chi, E. H.; Hashimoto, T.; Vinyals, O.; Liang, P.; Dean, J.; and Fedus, W. 2022. Emergent Abilities of Large Language Models. arXiv:2206.07682.

Wei, L.; Tan, Z.; Li, C.; Wang, J.; and Huang, W. 2024. Diff-eRank: A Novel Rank-Based Metric for Evaluating Large Language Models. arXiv:2401.17139.

Wu, B.; Xu, C.; Dai, X.; Wan, A.; Zhang, P.; Yan, Z.; Tomizuka, M.; Gonzalez, J.; Keutzer, K.; and Vajda, P. 2020. Visual Transformers: Token-based Image Representation and Processing for Computer Vision. arXiv:2006.03677.

Zhai, S.; Likhomanenko, T.; Littwin, E.; Busbridge, D.; Ramapuram, J.; Zhang, Y.; Gu, J.; and Susskind, J. 2023. Stabilizing transformer training by preventing attention entropy collapse. In *Proceedings of the 40th International Conference on Machine Learning*, ICML'23. JMLR.org.

Zhang, B.; and Sennrich, R. 2019. Root Mean Square Layer Normalization. arXiv:1910.07467.

Entropy-Lens: The Information Signature of Transformer Computations - Appendix

A Appendix Structure

The appendix is organized as follows:

- **Appendix B – Additional Experiments:** We assess the generality of our approach by applying it to Vision Transformers (ViTs). This analysis demonstrates that entropy profiles can be extracted and interpreted even in non-language domains, without any modification to our framework.
- **Appendix C – Evaluation Details:** We provide full details on the datasets and prompt templates used in our experiments. In particular, we specify how prompts were constructed for task classification, output correctness, and format classification tasks. This section also includes hardware information to support reproducibility.
- **Appendix D – Minimal Implementation:** We present a minimal code snippet that reproduces the core entropy profile extraction logic in a few lines of code. While our full codebase offers several optimizations and utilities, this section emphasizes transparency and ease of replication by showcasing the conceptual simplicity of our approach.

B Additional Experiments

To further test the generality and flexibility of our methodology, we conduct additional experiments beyond the core settings presented in the main text. In particular, we explore how Entropy-Lens performs in a different modality: computer vision. Without any architectural adjustment or fine-tuning, we apply the same framework to Vision Transformers (ViTs) and demonstrate that entropy profiles extracted from visual models exhibit meaningful and interpretable structure. This supports the claim that our method is not only scalable and model-agnostic, but also transferable across modalities.

B.1 Entropy-Lens for Vision Transformers

To demonstrate the versatility and robustness of our approach beyond language modeling, we analyze the entropy profiles of ViTs and DeiT.

Using 20 classes from ImageNet-1K (Russakovsky et al. 2015), with 20 images per class, and without any modifications to our framework, we generate the entropy profiles shown in Figure 8. We observe that all profiles start with high entropy values, which then decrease, mostly in the final layers. This behavior is qualitatively similar to that of GPTs or larger LLaMa models (Section 5.1), suggesting a *universal* pattern across domains as different as image processing and natural language processing.

Focusing on computer vision models, we note that while ViT and DeiT families exhibit qualitatively similar trends, they differ quantitatively—ViTs start with higher entropy values, making them easily distinguishable from DeiT.

Notably, the only profile that stands out is that of ViT Large (with ~ 300 M parameters), compared to the other models analyzed in this section, which have ≤ 86 M parameters.

For ViT Large, entropy decreases more smoothly, appearing not only as a better approximation of the sharp drop seen in smaller models but possibly following a different behavior entirely, with the entropy decline starting earlier.

We hypothesize a phase transition in entropy behavior as model size increases, occurring somewhere between 87M and 307M parameters.

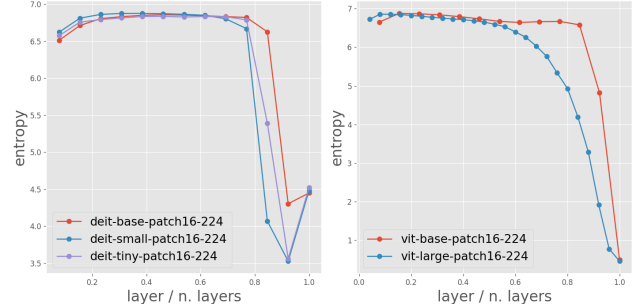


Figure 8: Entropy profiles for ViT model families.

C Evaluation Details

This section provides further details on the datasets and prompt templates used to evaluate the effectiveness of entropy profiles in the main experiments. In particular, we describe how we constructed the inputs for three key experimental settings: task type classification using the *TinyStories* dataset, correctness classification using the MMLU benchmark, and format classification using the *topic-format* dataset.

In all cases, prompt design plays a critical role in ensuring robust comparisons across experimental conditions. To this end, we employed multiple prompt variations. The subsections below report the full set of templates used, as referenced in Sections 5.2, 5.3, and 5.5 of the main paper.

The scripts used to generate these datasets—along with the full codebase to extract entropy profiles and reproduce all experiments—are shared as part of our code release.

Finally, we also provide information about the hardware used to run our experiments to facilitate reproducibility.

C.1 Prompt templates for TinyStories tasks

In Section 5.2, we describe an experimental setup designed to test whether entropy profiles can identify different types of tasks. To this end, we used the *TinyStories* dataset (Eldan and Li 2023) and constructed prompts combining short stories with specific task instructions. Each task type—*generative*, *syntactic*, and *semantic*—was associated with two distinct natural language formulations, referred to as task prompts. These are listed in Table 4. By varying the task prompt, we ensure that our classification results are not simply driven by surface-level textual artifacts, but instead reflect deeper computational signatures captured by the entropy profiles.

This table complements the prompt templates (base, reversed, and scrambled) described in the main text and pro-

vides the full set of instructions used to elicit different model behaviors.

Task Type	Task prompt
Generative	How can the story be continued? Which could be a continuation of the story?
Syntactic	How many words are in the story? Count the number of words in the story.
Semantic	What is the main idea of the story? Who is the subject of the story?

Table 4: Prompt templates used for *TinyStories* tasks.

C.2 Prompt templates for MMLU correctness classification

In Section 5.3, we test whether entropy profiles can distinguish between correct and incorrect answers produced by language models. To construct the dataset for this experiment, we used the Massive Multitask Language Understanding (MMLU) benchmark (Hendrycks et al. 2021), applying three distinct prompt styles to elicit different answer behaviors from the models. Table 5 reports the full prompt templates used in this experiment. Each template presents the same multiple-choice question in a different instructional format: the **Base** format presents the question directly; the **Instruct** format introduces an explicit instruction to select a single correct answer; and the **Humble** format includes an additional fallback directive encouraging the model to guess randomly if uncertain.

This variation in prompting allows us to control for instruction framing and to evaluate whether entropy profiles can capture response confidence and correctness robustly across different model behaviors. The table shown here complements the description in the main text.

C.3 Prompt Construction for the *Topic-Format* Dataset

To evaluate whether entropy profiles captures stylistic features of generated text, we constructed a custom dataset referred to as the *topic-format* dataset. In this setting, models are prompted to generate short texts on various topics, each constrained to adopt one of three specific formats: poem, scientific piece, or chat log. The goal is to determine whether these formats induce distinct entropy profiles, independently of the topic content.

We generated prompts by pairing 150 distinct topics with the following three format instructions:

- Write a poem about ...
- Write a scientific piece about ...
- Simulate a chat log about ...

Each prompt is constructed by concatenating a format prefix with a randomly selected topic (e.g., Write a poem about a planet). The resulting dataset contains 450 prompt completions per model, each paired with its entropy profile computed using Rényi entropy for $\alpha \in \{0.5, 1.0, 5.0\}$.

All generations were performed using a maximum generation length of 256 tokens. We then segmented the output into 8 equal-length windows and computed an entropy profile for each. The resulting data were stored with format labels and used in the classification and visualization tasks discussed in Section 5.5 of the main paper.

This setup enables robust testing of the extent to which entropy profiles encode formatting cues, beyond topical content or task semantics.

C.4 Experimental and hardware setup

All experiments were conducted on a compute node equipped with an NVIDIA L40 GPU, an Intel Xeon Gold CPU, 128 GB of RAM, and running Ubuntu 22.04. The primary software frameworks used were PyTorch, Transformer-Lens, and HuggingFace Transformers. Inference on LLMs was performed using float16 precision for improved efficiency.

D Minimal Implementation

To maximize reproducibility and transparency, we provide a minimal implementation of our framework. While our full codebase includes optimizations and utility functions to streamline analysis across models and datasets, the core idea behind Entropy-Lens is conceptually simple and can be expressed in just a few lines of code.

This section presents a compact example that computes the entropy profile of generated tokens using an off-the-shelf language model. Despite its brevity, this snippet captures the essence of our method: extracting intermediate representations, mapping them to vocabulary distributions, and computing their entropies.

D.1 Minimal Entropy Profile Extraction

The code in listing 1 demonstrates how to compute an entropy profile for a single prompt using a standard decoder-only transformer. It relies only on model forward passes and the use of logit-lens-style decoding. No gradients, fine-tuning, or access to internal model weights are required.

Prompt Type	Prompt
Base	<p>Subject: {subject}</p> <p>Question: {question}</p> <p>Choices:</p> <ul style="list-style-type: none"> A. {option_1} B. {option_2} C. {option_3} D. {option_4} <p>Answer:</p>
Instruct	<p>The following is a multiple-choice question about {subject}. Reply only with the correct option.</p> <p>Question: {question}</p> <p>Choices:</p> <ul style="list-style-type: none"> A. {option_1} B. {option_2} C. {option_3} D. {option_4} <p>Answer:</p>
Humble	<p>The following is a multiple-choice question about {subject}. Reply only with the correct option. If you are unsure about the answer, reply with a completely random option.</p> <p>Question: {question}</p> <p>Choices:</p> <ul style="list-style-type: none"> A. {option_1} B. {option_2} C. {option_3} D. {option_4} <p>Answer:</p>

Table 5: Prompt templates used for the MMLU dataset.

```

1 from transformers import AutoTokenizer, AutoModelForCausalLM
2 import torch
3
4 # Load GPT-2 and set up
5 tokenizer = AutoTokenizer.from_pretrained('gpt2')
6 model = AutoModelForCausalLM.from_pretrained('gpt2', device_map="auto").eval()
7 tokenizer.pad_token = tokenizer.eos_token
8
9 # Define entropy computation
10 ln, U = model.transformer.ln_f, model.lm_head
11 entropy = lambda x: -torch.sum(x * torch.log(x + 1e-15), dim=-1)
12
13 # Prepare input
14 input_text = 'The concept of entropy'
15 inputs = tokenizer.encode(input_text, return_tensors="pt").to(model.device)
16
17 # Generate with hidden states
18 outputs = model.generate(inputs,
19     do_sample=True,
20     max_new_tokens=32,
21     output_hidden_states=True,
22     return_dict_in_generate=True,
23     pad_token_id=tokenizer.pad_token_id
24 )
25
26 # Stack hidden activations and compute entropy signature
27 activations = torch.vstack([
28     torch.vstack(h).permute(1, 0, 2) for h in outputs.hidden_states
29 ])
30 entropy_signature = entropy(U(ln(activations)).softmax(dim=-1))

```

Listing 1: A minimal Python implementation of Entropy-Lens using Huggingface models and Pytorch.